Eur. Phys. J. B **2**, 183–190 (1998)

THE EUROPEAN PHYSICAL JOURNAL B

Electronic structural and magnetic properties of cadmium chalcogenide beryllosilicate sodalites

Y. Duan[a] and M. Jungen

Institute of Physical Chemistry, University of Basel, Klingelbergstrasse 80, 4056, Basel, Switzerland

Received: 28 March 1997 / Revised: 18 July 1997 / Accepted: 9 September 1997

Abstract. Density functional self-consistent spin-polarized calculations with the Discrete Variational Method were performed to obtain the electronic structures of cadmium chalcogenide beryllosilicate sodalites $Cd_8[BeSiO_4]_6Z_2$ and their bulk materials CdZ (Z = S, Se, Te). Similar as their bulk materials, these sodalites are also semiconductors. From their density of states and charge distributions, it was found that there is greater localization of the electron density in the sodalites compared with that of the bulk. The band gaps in their bulk compounds are different from those in the sodalite structures due to the electrons of Si, Be and O filled in. Different from their bulk materials, the d electrons of Cd play an important role to form an unseparated valence band with all orbitals of other elements. The calculated magnetic moments of these three materials are very small since all d atomic orbitals are fully occupied.

PACS. 71.20.-b Electron density of states and band structure of crystalline solids – 75.50.Ee Antiferromagnetics – 82.90.+j Other topics in physical chemistry

1 Introduction

Sodalites are a well-known class of anion containing framework consisting of β cages in zeolites. The composition of this class of material is very diverse. Most of them have the general formula $M_8[XYO_4]_6Z_n$ (n = 1, 2). For example, the anions Z incorporated into this formula include Cl^-, Br^-, I^-, SCN^-, OH^-, NO_2^-, NO_3^-, SO_4^{2-}, PO_4^{3-}, VO_4^{3-}, MnO_4^-, MoO_4^{2-}, CrO_4^{2-}, WO_4^{2-}, ClO_4^-, ClO_3^-, S_2^{2-}, CO_3^{2-}, $B(OH)_4^-$, $C_2O_4^{2-}$, $S_2O_3^{2-}$ *etc.* [1–4]. The structure diversity of the sodalite framework (X-Y) has been demonstrated widely. Of note are the Be-As frameworks [5], pure silica and aluminate sodalites [6–8], Al-Si and Al-Ge [1–3,9]; even more unusual is the phosphonitride sodalite framework of $Zn_7[P_{12}N_{14}]Cl_2$ synthesized by Schnick [10]. The sodalites are formed from $(XY)O_4$ tetrahedra, directly linked through the six-membered rings and containing a centrally placed anion coordinated tetrahedrally to four cations. Aluminate and borate sodalites have frameworks containing solely AlO_4 and BO_4 tetrahedra, with the general formula $M_8[XO_2]_{12}Z_2$ (X = Al, B), containing divalent cations and anions in the cavities [7,8]. Compositionally equivalent to these pure frameworks are the beryllosilicates, and the naturally occurring mineral genthelvite, $Zn_8[BeSiO_4]_6S_2$, is a member of this family [11]. These sodalites with more covalent entrapped ions are of interest as they may be considered to contain small blocks of (II,VI) semiconductors separated by the inert framework.

A lot of work has been done on the electronic properties of these sodalite structural materials. Moran *et al.* [12,13] investigated the compounds $Zn_8[BO_2]_{12}Z_2$, $M_8[BeSiO_4]_6Z_2$ (Z = S, Se, Te) and $Ga_xZn_{8-x}P_x[BO_2]_{12}Se_{2-x}$. They found that the optical absorption bands have a large blue-shift away from those of the bulk MZ materials and that the localization of the electron density in the sodalite is greater than in the bulk. Weller *et al.* [7,14] investigated $Cd_4[AlO_2]_6S_2$ and found that the individual M_4Z groups in these materials may have been electronically coupled and the shifted absorption maximum was probably due to small amounts of bulk CdS on the surface of the sodalite. Metiu *et al.* [15] studied the electronic and optical properties of dehydrated sodalite fully doped with Na and suggested that this system is a semiconductor due to a gap in its electronic structure. The same results are also obtained by Herron [16]. But their early work on sodalite saturated with alkali atoms shows that this system is a narrow band metal under the one-electron approximation [17]. Creighton *et al.* [18] simulated and interpreted the infrared and Raman spectra of sodalites $M_8[AlSiO_4]_6Cl_2$ (M = Li, Na, K) by the Wilson GF matrices. They found that the wavenumbers of their bands are simulated within 30 cm^{-1} and gave the relationships between the frequencies or intensities of the bands and the details of the structure of the sodalite framework.

Due to the structure of sodalites related to the well-known A-, X- and Y-type zeolites (see Fig. 1 in Ref. [15]), a large number of different sodalites have been

[a] *Present address*: School of Physics and Astronomy, University of Minnesota, 116 Church Street, SE. Minneapolis, MN 55455, USA. e-mail: duan@jwhp.spa.umn.edu

synthesized, and their compositions and structures have been characterized by chemical and thermal analysis, X-ray and neutron diffraction, and spectroscopic methods. Very recently, Weller *et al.* [19] synthesized a series of sodalites of the composition $Cd_8[BeSiO_4]_6Z_2$ (Z = S, Se, Te) and determined their structures by X-ray refinement and by IR and ^{29}Si MAS NMR spectra.

Although there are many theoretical studies on the zeolites [20–27], nevertheless there are still open questions concerning *e.g.* the detailed electronic structure of the nonframework constituents within the sodalite cage, the magnetic and conductive properties, and others. In this paper, the electronic structural and magnetic properties on the sodalites of $Cd_8[BeSiO_4]_6Z_2$ and the corresponding bulk materials CdZ (Z = S, Se, Te) are studied by density functional self-consistent spin-polarized calculations with the discrete variational method (DVM).

This paper is organized as follows: in the second section we briefly describe the theoretical method, in the third section we discuss the electronic structure results, and in the last section we summarize our conclusions.

2 Theoretical method

The discrete variational method (DVM) employed has been described in the original literature [28–31], here we give a summary and some details of the calculations. With the DVM, one solves the set of one-electron Kohn-Sham equations [32] of the density functional theory [33] in the local density approximation (in atomic units):

$$[-\frac{1}{2}\nabla^2 + V_{\rm c}(r) + V_{\rm xc}^{\sigma}(r) + V_{\rm ext}]\phi_{i\sigma}(r) = \epsilon_{i\sigma}\phi_{i\sigma}(r). \quad (1)$$

In equation (1), the Coulomb potential $V_{\rm c}$ includes electron-nucleus and electron-electron interactions, $V_{\rm ext}$ is an external potential which is used as the embedding potential around the cluster in our calculations, and $V_{\rm xc}^{\sigma}$ is the exchange-correlation potential of spin σ. In this paper we employed $V_{\rm xc}^{\sigma}$ as derived by von Barth and Hedin [34]. In the present spin-polarized calculations, the molecular orbitals $\phi_{i\sigma}$ are allowed to be different for each spin σ. The molecular potentials are functions of the electron density ρ_σ of spin σ:

$$\rho_\sigma(r) = \sum_i n_{i\sigma}|\phi_{i\sigma}|^2 \quad (2)$$

where $n_{i\sigma}$ is the occupation number of the molecular orbital $\phi_{i\sigma}$. The latter are expanded as linear combinations of symmetrized basis functions $\kappa(r)$,

$$\phi_{i\sigma}(r) = \sum_\mu C_{i\sigma}^{\mu}\kappa_\mu(r) \quad (3)$$

which in turn are expanded as linear combinations of numerical atomic orbitals χ_μ,

$$\kappa_\mu(r) = \sum_j D_{j\mu}\chi_\mu(r) \quad (4)$$

where $D_{j\mu}$ is the so-called symmetry coefficient which is determined only by the symmetry of the clusters. By minimization of the error functionals associated with each orbital $\phi_{i\sigma}$ in a three-dimensional grid of points, the secular equations are obtained:

$$[H][C] = [E][S][C] \quad (5)$$

in which the matrix elements are sums over the three-dimensional grid of points. Equation (5), in which $[H]$ is the Hamiltonian matrix, and $[S]$ is the overlap matrix, is solved self-consistently until a desired criterion is met up to a difference of $\leq 10^{-5}$ in the charge and spin densities.

In order to facilitate the computation of the electron-electron repulsion integrals, the molecular charge density was fitted to a multipolar expansion [35] with variation coefficients d_j:

$$\rho(r) \cong \sum_j d_j\rho_j(r) \quad (6)$$

where

$$\rho_j(r) = \sum_\nu^{I'}\sum_m C_{lm}^{\nu\lambda}R_N(r_\nu)Y_l^m(r_\nu). \quad (7)$$

In the above equation, j are atoms of a set I equivalent by symmetry; R_N, radial functions centered at atoms ν; and λ, a basis function associated to a particular value of l. The prime in the first summation indicates the restriction to atoms in the set I. In the present calculations, partial waves up to $l = 0$ were included for all atoms. The maximum least-squares error in the fit of ρ is 0.02 in our calculations.

The basis sets employed in our calculations are Cd[1s2s2p3s3p3d4s4p]4d5s5p; S[1s2s2p]3s3p3d; Se[1s2s2p3s3p3d]4s4p4d; Te[1s2s2p3s3p3d4s4p4d]5s5p5d; Si[1s2s2p]3s3p3d; Be[1s]2s2p and O[1s]2s2p. In order to save calculation time and disk space, a frozen core approximation was employed. All the shells consisting of orbitals bracketed in the above basis are kept in the core and unchanged during the iterations. The basis functions were improved; after convergence with a given set we obtained a new basis by performing calculations for the atoms with the configuration obtained in the molecular complexes. The atomic configurations were derived by Mulliken-type population analysis [36,37] in which the overlap population is divided proportional to the coefficient of the atom in the molecular orbital. The three-dimensional grid employed was divided into two regions: Around the nucleus is placed a sphere, where a precise polynomial integration is performed over a regular grid; outside of this sphere the points are generated by the pseudorandom Diophantine method [28–31]. In our calculations, the total number of the Diophantus sample points is 72000.

To obtain the electronic density of states (DOS) from the discrete energy levels ε_i, a Lorentzian expansion scheme is used and the total DOS is defined by

$$D(E) = \sum_{n,l,\sigma} D_{nl}^{\sigma}(E) \quad (8)$$

with

$$D^{\sigma}_{nl}(E) = \sum_i A^{\sigma}_{nl,i} \frac{\delta/\pi}{(E-\varepsilon_i)^2 + \delta^2} \tag{9}$$

where i labels the eigenfunctions and a broadening factor $\delta = 0.005$ a.u. is used in this paper. $A^{\sigma}_{nl,i}$ are the Mulliken population numbers [36,37], n and l are the orbital and angular quantum numbers.

3 Results and discussions

3.1 Cluster models

As Weller *et al.* [19] reported, for $Cd_8[BeSiO_4]_6Z_2$ (Z = S, Se, Te) crystals, all beryllosilicate structures were successfully refined in the space group $P\bar{4}3n$ (No. 218) demonstrating an ordering of the beryllium and silicon atoms in the framework. According to the space-group theory [38], Be and Si are positioned at the 6c and 6d sites, whereas O, Cd and Z are at the 24i, 8e and 2a sites respectively. That is the Be and Si are sited alternatively in the corners of the quadrilangle, between them connected with an oxygen atom, the Z atom is located in the center whereas the Cd atoms are approximately tetrahedrally coordinated to three framework oxides. According to the experimental results, a 77-atom cluster model was cut from their crystal structures which is shown in Figure 1a. This cluster contains 8 Cd atoms, 12 Be, 12 Si, 36 O and 9 Z (Z = S, Se, Te) atoms. There are -2 charges on this cluster. Around the cluster more than 1000 atoms are arranged to establish the embedding potential (V_{ext} of Eq. (1)). Different from the ideal sodalite structure, the O atom does not co-plane with the Be-Si plane; so this cluster model only belongs to the D_2 or C_{2V} point group. The coordinates of all the atoms in the cluster are taken from references [19,38].

In order to compare the results of this series of sodalites with their bulk materials, we also calculated their bulk materials CdZ (Z = S, Se, Te) with the same method and basis. As we know, CdZ (Z = S, Se) exists in two forms, Zinc Blende and Wurtzite, and CdTe only exists in the Zinc Blende form [39]. These two forms are closely related. Here we only calculated them in the form of Zinc Blende. In this form, the crystal constants are 5.818 Å, 6.077 Å and 6.481 Å for β-CdS, CdSe and CdTe respectively [39,40]. According to their crystal structures, the clusters $Cd_{38}Z_{44}$ (Z = S, Se, Te) were cut from their crystals as shown in Figure 1b. There are -12 charges on it. In this cluster each atom is symmetrically surrounded by four atoms of the other kind disposed at the corners of a regular tetrahedron. It is easy to find that this cluster belongs to the T_d point group. Similar as the $[Cd_8Be_{12}Si_{12}O_{36}Z_9]^{2-}$ cluster, around the $[Cd_{38}Z_{44}]^{12-}$ cluster, there are more than 1000 atoms forming the external embedding potential.

3.2 Electronic structure

In Table 1 are given the Mulliken-type occupation numbers of atomic orbitals (AOs) for each type of atoms

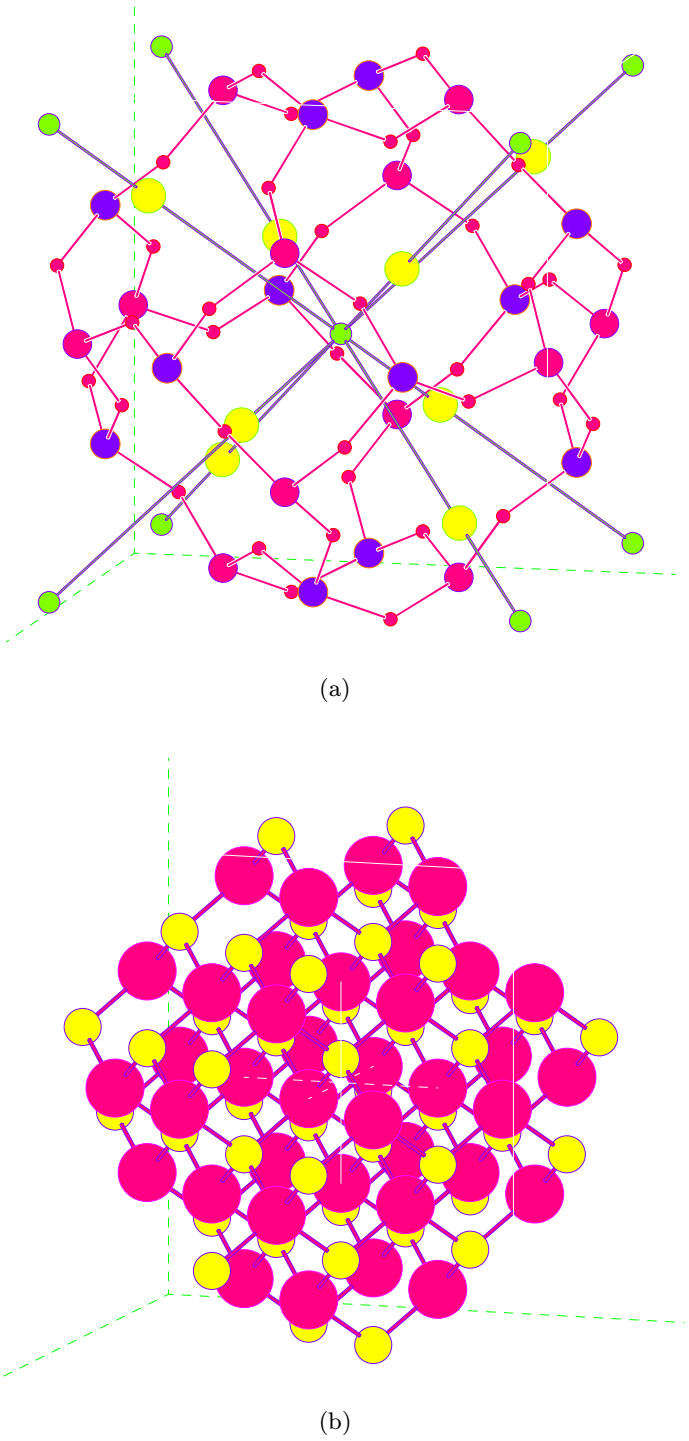

(a)

(b)

Fig. 1. Calculation models; (a) $Cd_8[BeSiO_4]_6Z_2$ (Z = S, Se, Te) systems which are modeled by $[Cd_8Be_{12}Si_{12}O_{36}Z_9]^{2-}$ clusters. The big dark balls are the Si and Be atoms which are alternatively sited, the small dark balls are O atoms, the big light balls are Cd atoms, and the small light balls are Z (Z = S, Se, Te) atoms; (b) CdZ (Z = S, Se, Te) systems which are modeled by $[Cd_{38}Z_{44}]^{12-}$ clusters. The dark balls stand for Cd atoms while the light balls are the Z atoms.

Table 1. The Mulliken-type populations, net charges and magnetic moments.

system	Mulliken population	Net charge	$\mu(\mu_B)$
$Cd_8[BeSiO_4]_6S_2$	Cd: 9.96(3d) 0.02(4s) 0.07(4p)	1.95	0.08
	S: 1.99(3s) 5.85(3p) 0.36(3d)	−2.20	0.03
	Si: 0.17(3s) 0.53(3p) 0.13(3d)	3.17	0.06
	Be: 0.03(2s) 0.16(2p)	1.81	0.00
	O: 1.99(2s) 5.72(2p)	−1.71	0.00
$Cd_8[BeSiO_4]_6Se_2$	Cd: 9.96(3d) 0.02(4s) 0.08(4p)	1.94	0.05
	Se: 1.99(4s) 5.84(4p) 0.42(4d)	−2.25	0.02
	Si: 0.12(3s) 0.37(3p) 0.10(3d)	3.41	0.03
	Be: 0.03(2s) 0.17(2p)	1.80	0.00
	O: 2.00(2s) 5.78(2p)	−1.78	0.00
$Cd_8[BeSiO_4]_6Te_2$	Cd: 9.96(3d) 0.03(4s) 0.09(4p)	1.92	0.03
	Te: 1.98(5s) 5.83(5p) 0.45(5d)	−2.26	0.01
	Si: 0.16(3s) 0.39(3p) 0.09(3d)	3.36	0.01
	Be: 0.04(2s) 0.19(2p)	1.77	0.00
	O: 1.99(2s) 5.74(2p)	−1.73	0.00
CdS	Cd: 9.95(3d) 0.02(4s) 0.08(4p)	1.95	0.00
	S: 1.98(3s) 5.68(3p) 0.32(3d)	−1.98	0.00
CdSe	Cd: 9.96(3d) 0.01(4s) 0.08(4p)	1.95	0.00
	Se: 1.98(4s) 5.74(4p) 0.26(4d)	−1.98	0.00
CdTe	Cd: 9.95(3d) 0.03(4s) 0.12(4p)	1.90	0.00
	Te: 1.98(5s) 5.69(5p) 0.26(5d)	−1.93	0.00

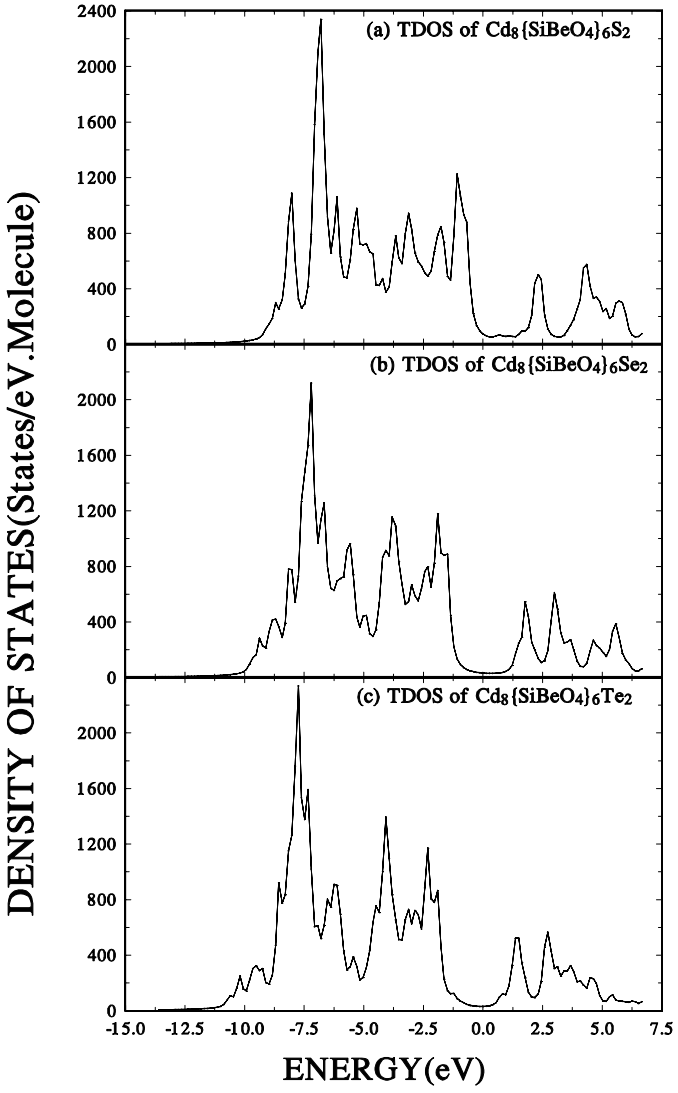

Fig. 2. The total density of states (TDOS) of $Cd_8[BeSiO_4]_6Z_2$ (Z = S, Se, Te). The Fermi level is taken as the relative energy zero point. (a) TDOS of $Cd_8[BeSiO_4]_6S_2$; (b) TDOS of $Cd_8[BeSiO_4]_6Se_2$; (c) TDOS of $Cd_8[BeSiO_4]_6Te_2$.

obtained from these three sodalites and their bulk materials. Since the differences between spin up and spin down are very small, only the sum of spin up and down is listed in Table 1. The net charges and magnetic moments μ, which is the sum of the differences of occupation between the spin up and spin down AO, are also listed in Table 1. From this table, it can be found that all six systems have very small magnetic moments which may be from the numerical noise. Therefore, they are antimagnetic materials. The populations of Cd and Z (Z = S, Se, Te) in the sodalite structures are nearly the same as in the bulk materials. The net charges of Cd and Z in their bulk materials are very close to 2.0, coinciding with their normal valence. But in the sodalite structure, although the net charge on Cd is nearly the same as in the bulk materials, the obtained charge on Z is larger than 2.0. The reason is that some charges are transferred from the sodalite framework onto Z atoms. The amounts of charge transfer of Si, Be and O in these three sodalite compounds are very close to each other.

Figure 2 shows the total DOS(TDOS) of $Cd_8[BeSiO_4]_6Z_2$ (Z = S, Se, Te). From this figure it can be seen that although the values of DOS are not exactly zero above the Fermi level (E_f), there is still an obvious gap. From the HOMO and LUMO orbital energies the obtained gap widths are 1.3 eV, 2.90 eV and 1.52 eV for $Cd_8[BeSiO_4]_6Z_2$ (Z = S, Se, Te) respectively. Therefore, these sodalite materials are semiconductors. Comparing Figures 2a, b and c one can see that the shapes of the DOS for these three systems are very similar to each other. Blake *et al.* [15] investigated the electronic properties of dehydrated sodalite fully doped with Na and obtained a band gap of 1.09 eV. Monnier *et al.* [17] studied the electronic properties of sodalite saturated with alkali atoms and suggested that the system is a narrow band metal under the one-electron approximation and is antiferromagnetic at low

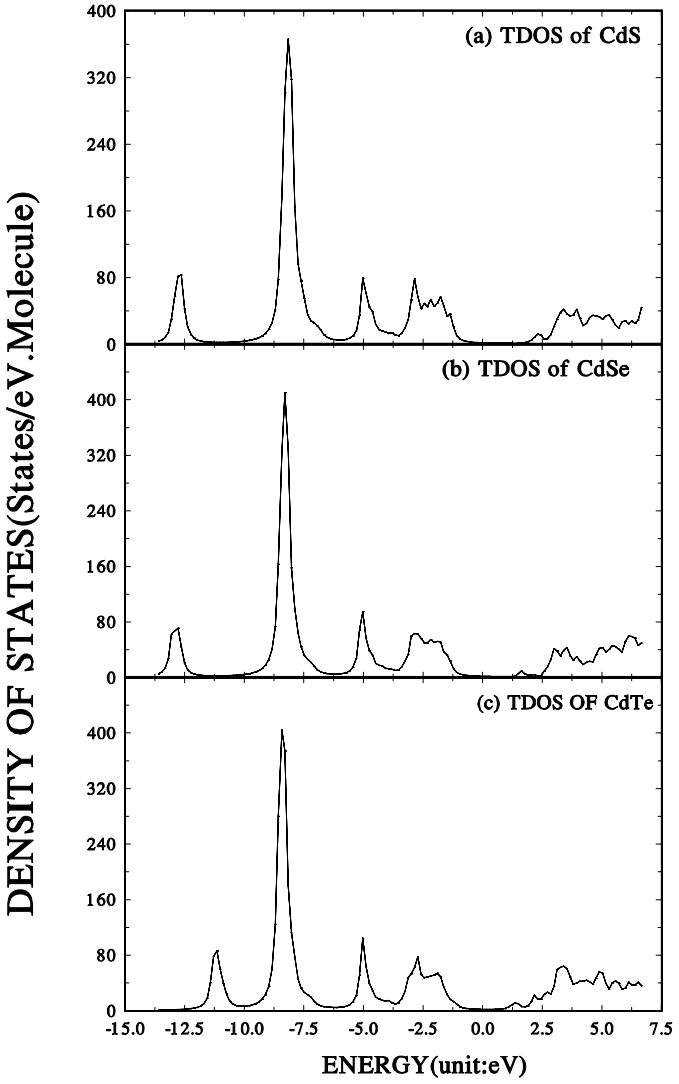

Fig. 3. TDOS of $Cd_{38}Z_{44}$ (Z = S, Se, Te): (a) TDOS of CdS; (b) TDOS of CdSe; (c) TDOS of CdTe.

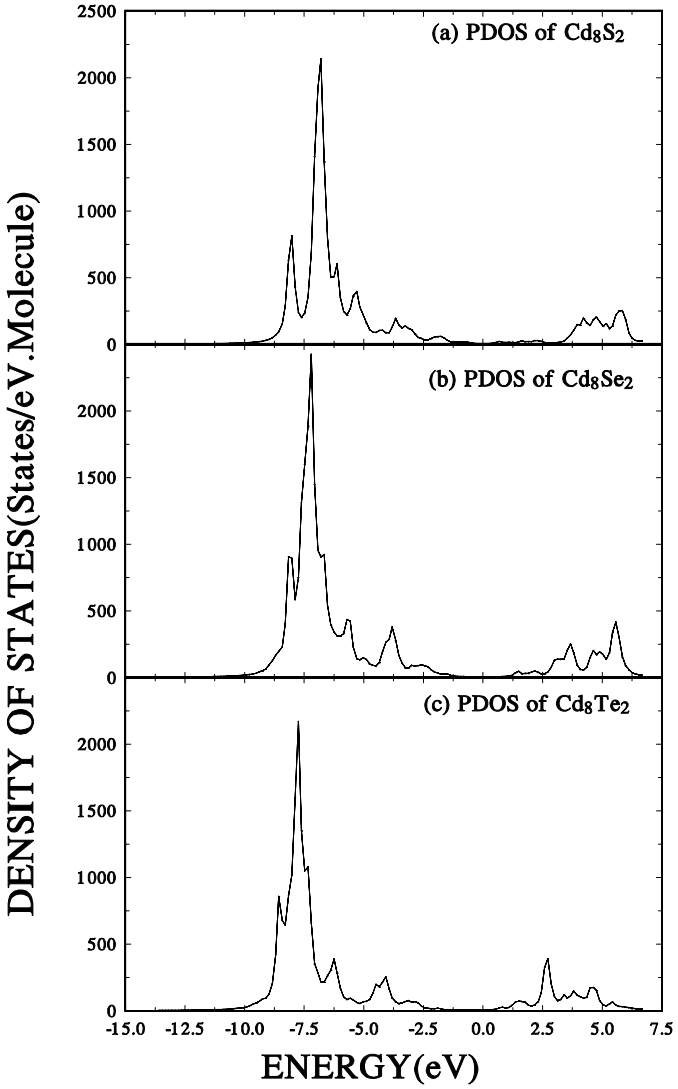

Fig. 4. Partial density of states (PDOS) of Cd_8S_2 cluster in $Cd_8[BeSiO_4]_6Z_2$ (Z = S, Se, Te): (a) PDOS of Cd_8S_2; (b) PDOS of Cd_8Se_2; (c) PDOS of Cd_8Te_2.

temperature. Up to now we have not found any calculated or experimental results for our calculated systems since they are newly synthesized materials [19]. From our present calculation, although we could not obtain the exact band gap due to the cluster approximation, they are certainly semiconductors similar as their bulk materials.

In order to compare the TDOS of sodalite structure materials to their bulk materials, Figure 3 shows the calculated TDOS of their bulk materials CdZ (Z = S, Se, Te). This figure is very similar as that of their corresponding sodalite materials (Fig. 2). From the calculated magnetic moments listed in Table 1, they are also antimagnetic materials. From the calculated HOMO and LUMO eigenvalues, the obtained band gaps are 2.61 eV, 2.65 eV and 1.35 eV for CdZ (Z = S, Se, Te) respectively. The calculated band gap of CdS is in agreement with experimental results of 2.50 eV [41], 2.55 eV [42] and with band theory results of 2.44 eV [43], 2.51 eV [44]. The obtained band gap of CdTe is also close to the experimental result 1.60 eV [45] and the band theory results of 1.60 eV [44], 1.56 eV [43]. But the value for CdSe is far away from the experimental results of 1.79 eV [43], 1.84 eV [45], 1.666 eV [46] and from the band theory results of 1.60 eV [44], 1.56 eV [43]. The reason may be that our cluster size is not enough large and the local spin density approximation are used in DVM.

In Figure 4 are shown the partial DOS(PDOS) of the Cd_8Z_2 cluster in the sodalite $Cd_8[BeSiO_4]_6Z_2$ (Z = S, Se, Te). Comparing Figure 4 with Figure 3, it can be seen that in the bulk materials (Fig. 3) the TDOS consists of 4 separated peaks below the Fermi level and the energy range is extended to 12.0 eV, whereas in the sodalite materials, the PDOS of Cd_8Z_2 are constrained together to form an unseparated peak. The energy range is extended only to about 7.0 eV and the maxima of the DOS are closer to their Fermi level. Therefore there is greater electron density localization in the sodalite compared to

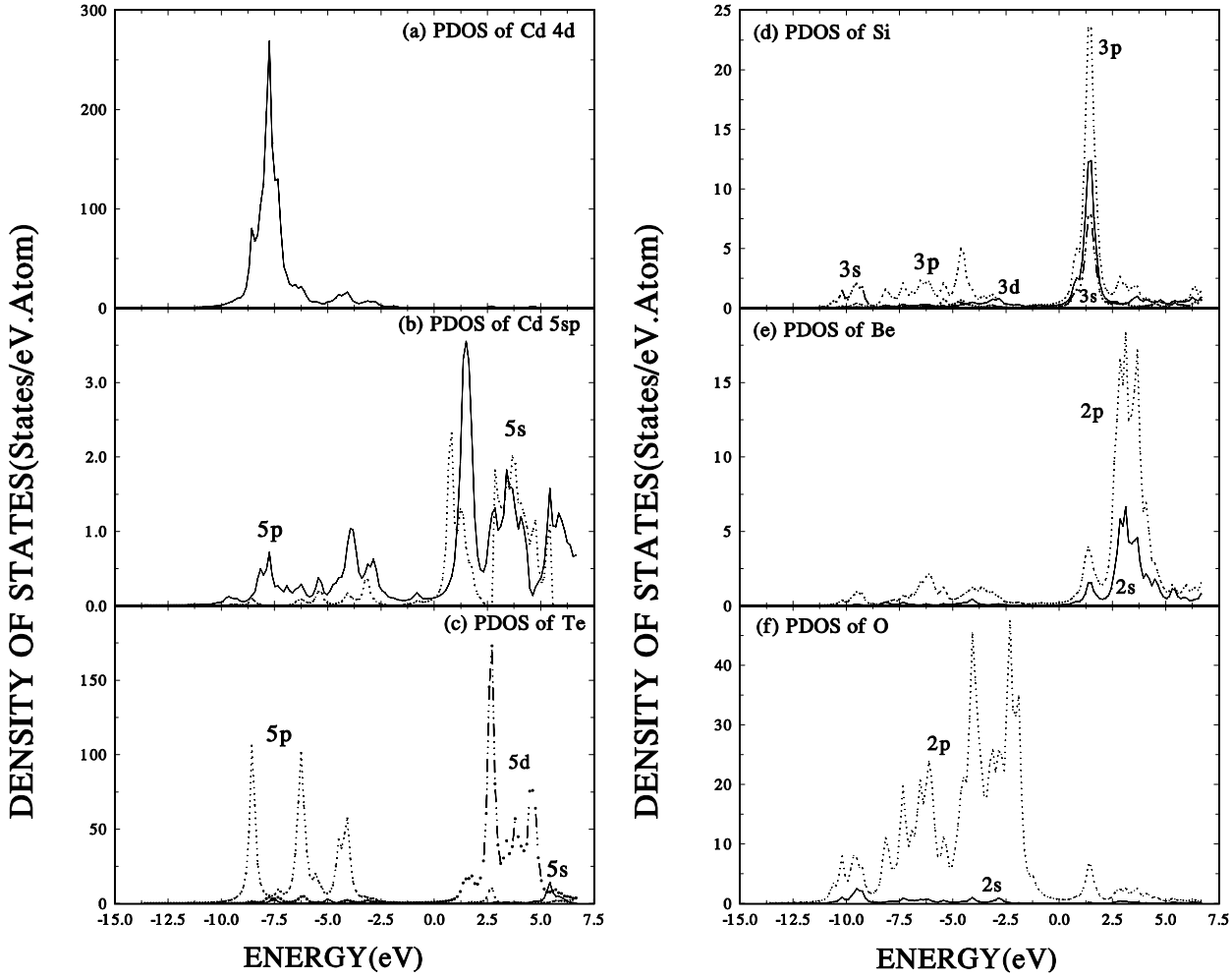

Fig. 5. PDOS of Cd, Te, Si, Be and O in $Cd_8[BeSiO_4]_6Te_2$: (a) PDOS of the 3d orbitals of Cd; (b) PDOS of the 4s and 4p orbitals of Cd; (c) PDOS of Te; (d) PDOS of Si; (e) PDOS of Be; (f) PDOS of O.

the bulk. This conclusion is in agreement with the results of optical absorption bands and with MAS NMR spectra by Moran *et al.* [12,13]. In bulk material, one Cd is surrounded by four Z atoms and around each Z atom there are four Cd atoms. But in sodalite, the coordination is changed. Around one Z atom there are four closest Cd atoms, but to each Cd atom only one Z atom is directly connected. Therefore the PDOS of Cd_8Z_2 (Fig. 4) is very different from the TDOS of bulk materials (Fig. 3).

From the above results, all these three sodalites have similar properties. As an example, Figures 5 and 6 show all the PDOS of each atom type in the sodalite structure $Cd_8[BeSiO_4]_6Te_2$ and its bulk material modeled by $Cd_{38}Te_{44}$. Comparing Figure 2c with Figures 5a, b and c, it can be seen that in the sodalite $Cd_8[BeSiO_4]_6Te_2$ the d orbital of Cd play an important role for the bonding with the 5p orbital of Te and the 2p orbital of O (Fig. 5f) and 3sp orbitals of Si (Fig. 5d). Its 5sp orbitals have only small contributions around the Fermi level. Comparing them with Figure 6, we see some differences. In the bulk material CdTe the 4d of Cd and 5s of Te simply formed two single separate bands (see also Fig. 3c), the 5sp orbitals of Cd bonded with 5p and 5d orbitals of Te and formed other two bands. But in sodalite structure, the 4d orbitals of Cd with its 5sp orbitals bonded with 5p of Te and 2p of O and all the orbitals of Si and Be to form an unseparated valence band (see Fig. 2c). In the bulk CdTe (Fig. 6), the 5s of Te has an obvious contribution and formed a single band, its 5p bonded with 5p of Cd, its 5d orbitals and 5s of Cd have larger contributions to the conductive band (CB) rather than to the valence band (VB). In the sodalite material (Fig. 5), in the same energy range the 5s of Te has a very small contribution to the VB and CB, its 5d has a larger contribution to the CB than to the VB, the mainly bonding orbitals of Te are its 5p. From Figures 5d, e and f it can be seen that the orbitals of Si and Be are bonded with the 2p orbital of O and form the sodalite framework. The 2p of O has a much larger contribution in the VB than in CB. Comparing Figure 5 with Figure 6 one can see that above the Fermi level in the sodalites there are much larger contributions from all the orbitals of Be, Si and O (see also Fig. 2). This means that the electrons of the framework are filled into

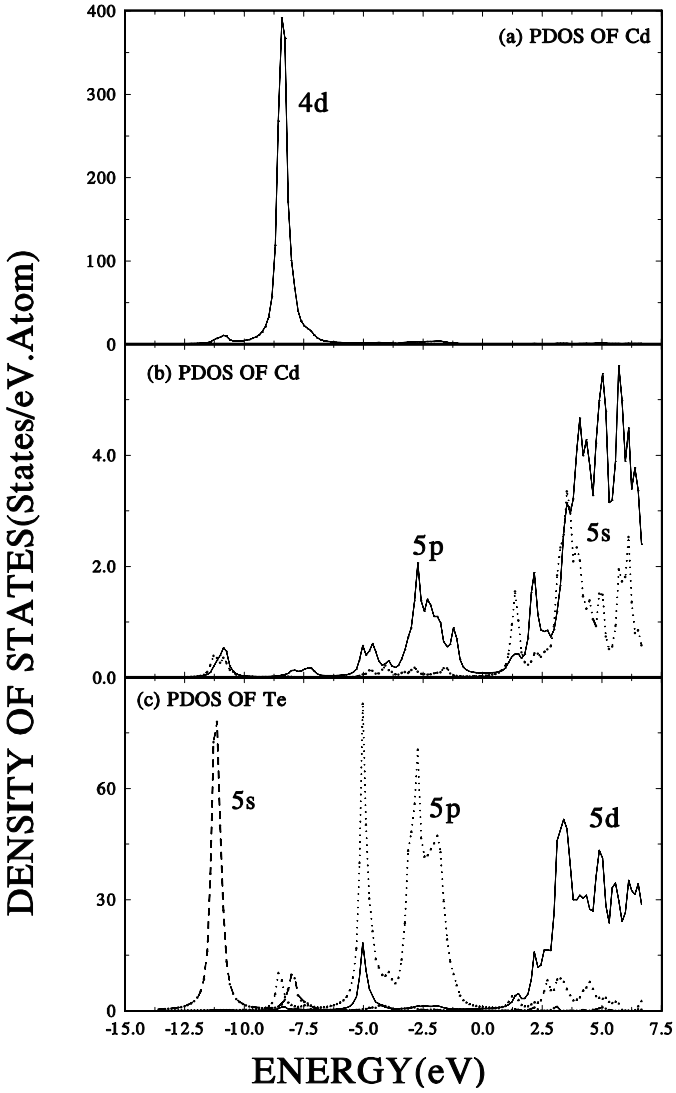

Fig. 6. PDOS of Cd and Te in CdTe: (a) PDOS of the 3d orbitals of Cd; (b) PDOS of the 4s and 4p orbitals of Cd; (c) PDOS of Te.

the non-bonding orbitals which results in a non-vanishing DOS of the sodalites in this energy range.

4 Summary and conclusions

In this paper we have calculated the electronic and magnetic properties of cadmium chalcogenide beryllosilicate sodalites $Cd_8[BeSiO_4]_6Z_2$ and their bulk materials CdZ (Z = S, Se, Te). Like the corresponding bulk materials, the sodalites are also semiconductors. From their density of states and charge distributions, it was found that there is greater electron density localization in the sodalites compared to the bulk. The band gaps in their bulk compounds are different from those in the sodalite structures due to the electrons of Si, Be and O filled in. In bulk materials, the 4d electrons of Cd and the s electron of Z formed two separated bands because in this energy range the contributions of orbitals of other elements are very small; other bands are formed by the 5sp orbitals of Cd bonding with all p and d orbitals of Z. In sodalite structures, the 4d electrons of Cd play an important role to form the whole valence band together with all orbitals of other elements. The calculated magnetic moments of these materials are very small since all d atomic orbitals are fully occupied.

This work is part of the project Nr. 20-43383-95 of Schweizerischer Nationalfonds. The authors thank Mr. P. Rapp for his useful help on the calculations.

References

1. R.M. Barrer, J.F. Cole, H.J. Villiger, Chem. Soc. A, 1524 (1970).
2. F.Z. Hund, Anorg. Allg. Chem. **511**, 225 (1984).
3. M.T. Weller, K. Haworth, J. Chem. Soc. Commun. **10**, 734 (1991).
4. G. Engelhardt, J. Felsche, P. Sieger, J. Am. Chem. Soc. **114**, 1173 (1992).
5. W.T.A. Harrison, T.E. Gier, G.D. Stucky, Acta Crystallogr. **C50**, 471 (1994).
6. D.M. Bibby, M.P. Dale, Nature **317**, 157 (1985).
7. G. Blasse, G.J. Dirksen, M.E. Brenchley, M.T. Weller, Chem. Phys. Lett. **234**, 177 (1995).
8. M.E. Brenchley, M.T. Weller, J. Mater. Chem. **2**, 1003 (1992).
9. M.E. Fleet, Acta Crystallogr. **C45**, 843 (1989).
10. W. Schnick, J.Z. Lücke, Anorg. Allg. Chem. **620**, 2014 (1994).
11. I. Hassan, H.D. Grundy, Am. Mineral. **70**, 186 (1985).
12. K.L. Moran, W.T.A. Harrison, T.E. Gier, Mater. Res. Soc. Symp. Proc. **164**, 123 (1990); **242**, 249 (1992).
13. K.L. Moran, W.T.A. Harrison, T.E. Gier, W. Ott, H. Eckert, K. Eichele, R.E. Wasylishen, G.D. Stucky, J. Am. Chem. Soc. **115**, 10553 (1993).
14. M.E. Brenchley, M.T. Weller, Angew. Chem. Int. Ed. Engl. **32**, 1663 (1993).
15. N.P. Blake, V.I. Srdanov, G.D. Stucky, H. Metiu, J. Chem. Phys. **104**, 8721 (1996).
16. N. Herron, Y. Wang, M.M. Eddy, G.D. Stucky, D.E. Cox, K. Moller, T. Bein, J. Am. Chem. Soc. **111**, 530 (1989).
17. A. Monnier, V.I. Srdanov, G.D. Stucky, H. Metiu, J. Chem. Phys. **100**, 6944 (1994).
18. J.A. Creighton, H.W. Deckman, J.M. Newsam, J. Phys. Chem. **98**, 448 (1994).
19. S.E. Dann, M.T. Weller, Inorg. Chem. **35**, 555 (1996).
20. T. Fujino, M. Kashitani, J.N. Kondo, K. Domen, C. Hirose, J. Phys. Chem. **100**, 11649 (1996).
21. C.J.A. Mota, P.M. Esteves, M.B. de Amorim, J. Phys. Chem. **100**, 12418 (1996).
22. M. Mabilia, R.A. Pearlstein, A.J. Hopfinger, J. Am. Chem. Soc. **109**, 7960 (1987).
23. V.A. Ermoshin, K.S. Smirnov, D. Bougeard, Chem. Phys. **209**, 41 (1995).
24. J.R. Hill, J. Sauer, J. Phys. Chem. **98**, 1238 (1994); **99**, 9536 (1995).
25. F. Filippone, F. Buda, S. Iarlori, G. Moretti, P. Porta, J. Phys. Chem. **99**, 12883 (1995).
26. K.P. Schröder, J. Sauer, J. Phys. Chem. **100**, 11043 (1996).

27. J. Sauer, R. Zahradnik, Int. J. Quantum Chem. **26**, 793 (1984).
28. D.E. Ellis, Int. J. Quantum Chem. **S2**, 35 (1968).
29. D.E. Ellis, G.S. Painter, Phys. Rev. **B2**, 2887 (1970).
30. F.W. Averill, D.E. Ellis, J. Chem. Phys. **59**, 6412 (1973).
31. E.J. Baerends, D.E. Ellis, P. Ros, Chem. Phys. **2**, 41 (1973).
32. W. Kohn, L.J. Sham, Phys. Rev. **A140**, 1133 (1965).
33. R.G. Parr, W. Yang, *Density Functional Theory of Atoms and Molecules* (Oxford University Press, New York, 1989).
34. U. von Barth, L. Hedin, J. Phys. **C5**, 1629 (1972).
35. B. Delley, D.E. Ellis, J. Chem. Phys. **76**, 1949 (1982).
36. R.S. Mulliken, J. Chem. Phys. **23**, 1833 (1955).
37. C. Umrigar, D.E. Ellis, Phys. Rev. **B21**, 852 (1980).
38. *International Tables for Crystallography*, edited by Hahn, Theo, Vol. A (Kluwer Academic Publishers, 4-th ed., 1995).
39. T.C.W. Mak, G.D. Zhou, *Crystallography in Modern Chemistry* (John Willey & Sons, Inc., 1992).
40. R.W.G. Wyckoff, Crystal Structures, 2nd ed., Vol. 1 (Willey-Interscience, New York, 1971).
41. Y. Kayanuma, Phys. Rev. **B38**, 9797 (1988).
42. M. Cardona, M. Weinstein, G.A. Wolff, Phys. Rev. **A140**, 633 (1965).
43. A. Tomasulo, M.V. Ramakrishna, J. Chem. Phys. **105**, 3612 (1996).
44. M. Huang, W.Y. Ching, J. Phys. Chem. Solids **46**, 977 (1985).
45. W.A. Harrison, *Electronic Structure and the Properties of Solids* (Freeman, San Francisco, 1980).
46. Y.D. Kim, M.V. Klein, S.F. Ren, Y.C. Chang, H. Luo, N. Samarth, J.K. Furdyna, Phys. Rev. **B49**, 7262 (1994).